Phosphaferrocenes

DOI: 10.1002/anie.201403581

# Functionalization of a *cyclo*-$P_5$ Ligand by Main-Group Element Nucleophiles**

*Eric Mädl, Mikhail V. Butovskii, Gábor Balázs, Eugenia V. Peresypkina, Alexander V. Virovets, Michael Seidl, and Manfred Scheer**

*Dedicated to Professor Otto Scherer on the occasion of his 80th birthday*

***Abstract:*** *Unprecedented functionalized products with an $\eta^4$-$P_5$ ring are obtained by the reaction of [Cp*Fe($\eta^5$-$P_5$)] (**1**; Cp* = $\eta^5$-$C_5Me_5$) with different nucleophiles. With $LiCH_2SiMe_3$ and $LiNMe_2$, the monoanionic products $[Cp^*Fe(\eta^4\text{-}P_5CH_2SiMe_3)]^-$ and $[Cp^*Fe(\eta^4\text{-}P_5NMe_2)]^-$, respectively, are formed. The reaction of **1** with $NaNH_2$ leads to the formation of the trianionic compound $[\{Cp^*Fe(\eta^4\text{-}P_5)\}_2N]^{3-}$, whereas the reaction with $LiPH_2$ yields $[Cp^*Fe(\eta^4\text{-}P_5PH_2)]^-$ as the main product, with $[\{Cp^*Fe(\eta^4\text{-}P_5)\}_2PH]^{2-}$ as a byproduct. The calculated energy profile of the reactions provides a rationale for the formation of the different products.*

Ferrocene, the first organometallic sandwich complex, which was discovered over 60 years ago,[1] has proven to be a versatile and significant compound in chemistry. Whereas in the beginning of the ferrocene chemistry, extensive reactivity studies were performed,[2] it is currently widely used for polymer chemistry,[3] for asymmetric catalysis,[4] or for medical applications.[5] One of the most striking reactions of ferrocene is its reaction with strong organometallic bases, such as organolithium compounds,[6,7] which lead to the deprotonation of the $C_5H_5$ unit and the formation of mono- and dilithioferrocenes. This demonstrates that the reactivity pattern of ferrocene towards nucleophiles is dominated by the $C_5H_5$ ligands. The most analogous polyphosphorus derivative is pentaphosphaferrocene [Cp*Fe($\eta^5$-$P_5$)] (Cp* = $\eta^5$-$C_5Me_5$) (**1**).[8] We and the Scherer group have been interested in the reactivity of **1**, and it has been shown that the *cylco*-$P_5$ unit can coordinate to transition-metal carbonyl species to give triple-decker complexes and other subsequent organometallic compounds containing distorted $P_5$ units,[9] and to copper(I) halides to give 1D and 2D polymers[10] or even spherical fullerene-like superballs.[11] The redox chemistry of **1** was initially investigated by Winter and Geiger,[12] and only recently we were able to isolate and characterize the dicationic species $[(Cp^*Fe)_2(\mu,\eta^{4:4}\text{-}P_{10})]^{2+}$, as well as the dianionic species $[(Cp^*Fe)_2(\mu,\eta^{4:4}\text{-}P_{10})]^{2-}$ and [Cp*Fe($\eta^4$-$P_5$)]$^{2-}$.[13] However, what is missing in the chemistry of **1** is its reactivity towards main-group nucleophiles to develop a better understanding of its reaction chemistry in comparison to its carbonaceous relative ferrocene. Density functional theory calculations on **1** show that the LUMO and LUMO + 1 orbitals are mostly localized on the P atoms of the *cyclo*-$P_5$ ligand and the positive charge is also located there.[14] Therefore, it can be assumed that nucleophilic attack can occur at the *cyclo*-$P_5$ ligand. Herein, we report the first reactivity of pentaphosphaferrocene towards main-group nucleophiles, leading to an unprecedented functionalization of the *cyclo*-$P_5$ ligand. With these first results, this molecule is now becoming a valuable starting material in organometallic-based main-group chemistry.

Mixing a green solution of **1** and $LiCH_2SiMe_3$ or $LiNMe_2$ in diethyl ether or THF at low temperatures resulted in immediate color change to dark brown to give, after work-up, [Li($Et_2O$)][**2**] (92% yield) or [Li(THF)$_4$][**3**] (51% yield) (Scheme 1). The $^{31}$P NMR spectra of **2** and **3** show an AMM′XX′ spin system with resonances centered at −56.0, 13.2, and 76.5 ppm and at −32.4, 23.9, and 119.7 ppm, respectively. Whereas for **2** crystals of suitable quality could

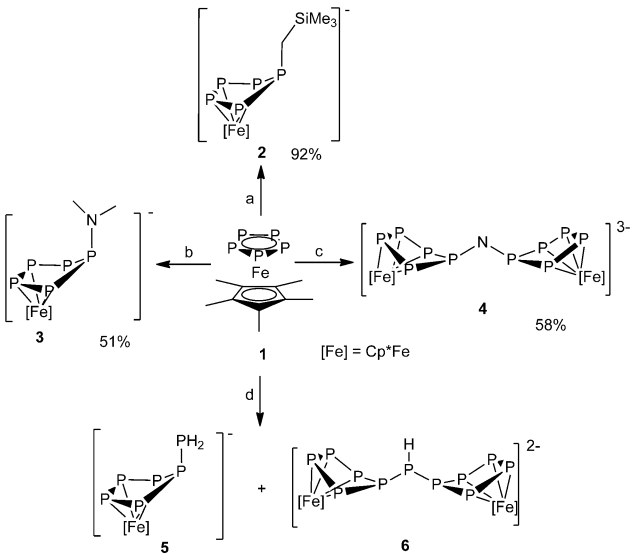


***Scheme 1.*** Reactivity of **1** towards nucleophiles: a) $LiCH_2SiMe_3$ in $Et_2O$, −35 °C→RT; b) $LiNMe_2$ in THF, −35 °C→RT; c) $NaNH_2$ in dme, RT; d) $LiPH_2$ in THF, −60 °C→RT.

[*] E. Mädl, Dr. M. V. Butovskii, Dr. G. Balázs, M. Seidl, Prof. Dr. M. Scheer
University of Regensburg, Institut für Anorganische Chemie
93040 Regensburg (Germany)
E-mail: manfred.scheer@ur.de
Dr. E. V. Peresypkina, Dr. A. V. Virovets
Institute of Inorganic Chemistry SB RAS
Ak. Lavrentiev prosp. 3, Novosibirsk 630090 (Russia)

[**] This work was supported by the Deutsche Forschungsgemeinschaft.
Supporting information for this article is available on the WWW under http://dx.doi.org/10.1002/anie.201403581.

  

be obtained, all attempts to get such crystals for $[Li(THF)_4]$[**3**] failed, and its X-ray structure analysis was impeded by intrinsic disorder of the Cp* and $\eta^4$-$\{P_5(NMe_2)\}$ groups over alternative positions prevented a satisfying determination of the structural parameters. However, the atom connectivity of **3** was unambiguously determined being similar to that one found for **2**. The X-ray structural analysis of $[Li(Et_2O)]$[**2**], which represents a Li bridged dimer $\{[Li(Et_2O)_2][\mathbf{2}]\}_2$ in the solid state, shows an $\eta^4$-$P_5$ ring of the former *cyclo*-$P_5$ unit in envelope conformation with the $CH_2SiMe_3$ group being attached to the phosphorus atom which is bent out of the plane from the $\eta^4$-$P_5$ ring (Figure 1). All P–P bonds show

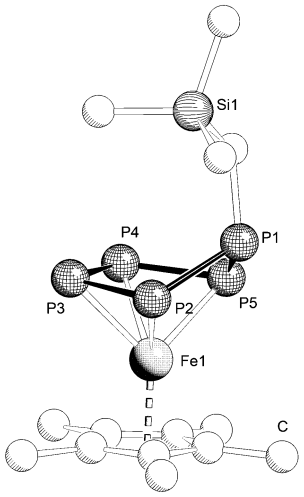


***Figure 1.*** Molecular structure of the anion of $[Li(Et_2O)]$[**2**]. H atoms are omitted for clarity. Selected bond lengths [Å] and angles [°]: P1–P2 2.1663(9), P1–P5 2.1569(9), P2–P3 2.1466(10), P3–P4 2.1342(11), P4–P5 2.1535(9), P1–C1 1.843(3), Fe1–P2 2.3218(8), Fe1–P3 2.3350(8), Fe1–P4 2.3420(8), Fe1–P5 2.3040(7); P5-P1-P2 92.81(4), P3-P2-P1 106.53(4), P4-P3-P2 103.91(4), P3-P4-P5 102.90(4), P4-P5-P1 106.93(4).

double-bond character (2.1299(10)–2.1623(8) Å), while the nearly planar $P_4$ unit is coordinating almost symmetrically to the Cp*Fe fragment. Apart from **2** and the other products **3**–**6** herein and former reported oxidation/reduction products of **1**,[13] only very few compounds are known containing *cyclo*-$P_5$ ligands in envelope conformation, coordinating in a $\eta^4$-manner to a transition metal. One of these rare examples is the niobium complex $[Na(THF)_6][\{Ar(Np)N\}(\eta^4\text{-}P_5)Nb\{N(Np)Ar\}_2]$ ($Np = CH_2tBu$; $Ar = 3,5\text{-}Me_2C_6H_3$) reported recently by Cummins et al.[15] The bond lengths of **2** are in the same range as in the above-mentioned compounds.

By using the parent $NH_2^-$ nucleophile, despite several attempts, we were not able to isolate a monoanionic compound. However, brown crystals containing the trianion **4** could be isolated in 58% yield (Scheme 1).[16] The $^{31}P$ NMR spectrum of **4** shows an AA′XX′X″X‴YY′Y″Y‴ spin system with three multiplets centered at −0.5, 13.8, and 149.6 ppm. The X-ray structural analysis of $[Na_3(dme)_5]$[**4**] (Figure 2; dme = 1,2-dimethoxyethane) reveals that two $[Cp^*FeP_5]$ fragments are linked by one nitrogen atom, resulting in the trianionic unit $[\{Cp^*Fe(\eta^4\text{-}P_5)\}_2N]^{3-}$. The P–P bonds are

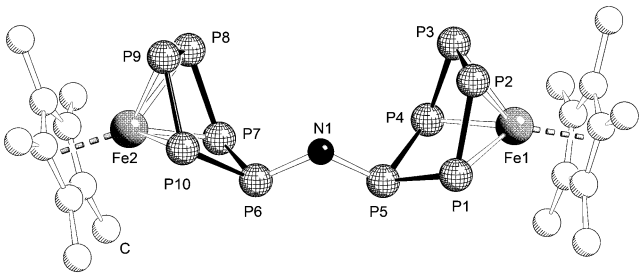


***Figure 2.*** Molecular structure of the anion of $[Na_3(dme)_5]$[**4**]. H atoms are omitted for clarity. Selected bond lengths [Å] and angles [°]: P1–P5 2.1700(13), P1–P2 2.1843(18), P2–P3 2.156(3), P3–P4 2.1411(19), P4–P5 2.1785(14), P6–P10 2.1614(13), P6–P7 2.1837(14), P7–P8 2.1593(18), P8–P9 2.136(2), P9–P10 2.1611(17), P1–Fe1 2.3026(11), P2–Fe1 2.2988(12), P3–Fe1 2.3157(13), P4–Fe1 2.3237(12); P5-P1-P2 106.80(6), P3-P2-P1 102.49(6), P4-P3-P2 102.51(6), P3-P4-P5 108.21(7), N1-P5-P1 110.77(11), N1-P5-P4 112.00(11), P5-N1-P6 116.77(17).

similar to those of **2**. The P–N bonds are in the expected range of a P–N single bond (P5–N1 1.688(3) Å, P6–N1 1.692(3) Å).

The formation of **4** can be rationalized as follows: The first step of the reaction is a nucleophillic attack of $NH_2^-$ leading to the formation of **A** (Scheme 2). Because $NH_2^-$ is also

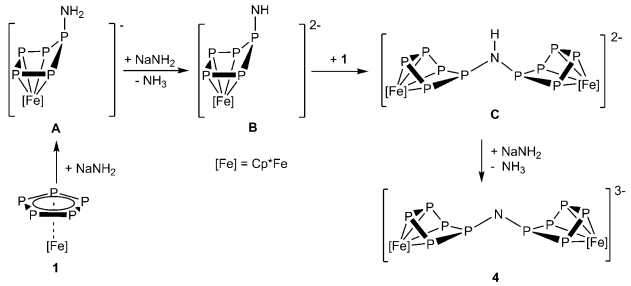


***Scheme 2.*** Proposed pathway for the formation of **4**.

a strong base it can deprotonate **A** to give **B**, which reacts with a further molecule of **1** to form the dianionic species **C**. The subsequent deprotonation of **C** by $NH_2^-$ gives the final product **4**. The formation of the intermediates **A** and **C** was monitored by $^{31}P$ NMR spectroscopy. When a $^{31}P$ NMR spectrum of the reaction mixture is recorded after 30 min, two sets of signals can be observed for $[Cp^*Fe(\eta^4\text{-}P_5)NH_2]^-$ (**A**) and $[\{Cp^*Fe(\eta^4\text{-}P_5)\}_2NH]^{2-}$ (**C**), respectively. Note that **4** has not formed at this stage yet and **1** is still present in the reaction mixture. After another three days, all sets of signals corresponding to **A** and **C** have disappeared and only the signals corresponding to **4** as well as some decomposition products are observed. The long reaction time is caused by the poor solubility of $NaNH_2$. According to DFT calculations, the reaction of **1** with $NH_2^-$ and the deprotonation of **A** by $NH_2^-$ are exothermic in solution by $-190.1\ kJ\,mol^{-1}$ and $-30.0\ kJ\,mol^{-1}$, respectively. Both the reaction of **B** with **1** and the deprotonation of **C** by $NH_2^-$ are exothermic in solution by $-134.5\ kJ\,mol^{-1}$ and $-17.4\ kJ\,mol^{-1}$, respectively (Figure 3). Although there is a large difference between the relative energies of **1** and **4**, intermediates **A** and **C** can be

  

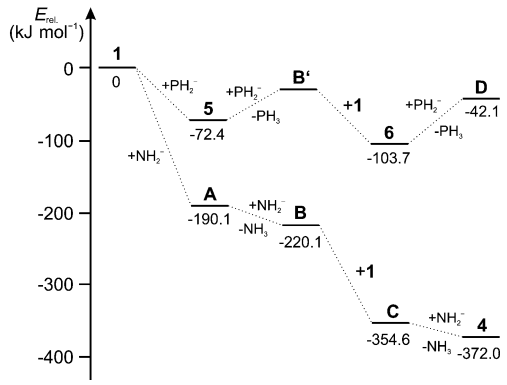


***Figure 3.*** Energy profile of the formation of **4**, **5**, and **6**.

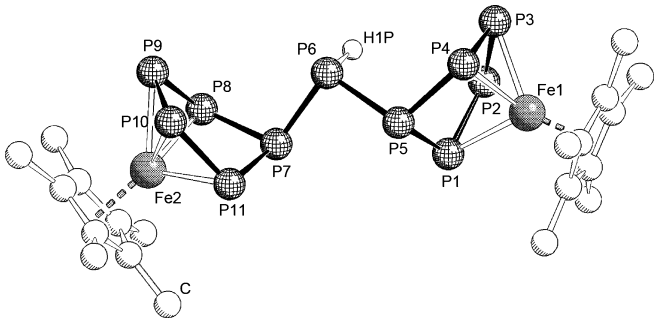


***Figure 4.*** Molecular structure of the anion of $[Li_2(dme)_6][\mathbf{6}]$. Li atoms, coordinated dme, and H atoms are omitted for clarity. Selected bond lengths [Å] and angles [°]: P1–P2 2.1537(15), P1–P5 2.1669(14), P2–P3 2.1327(15), P3–P4 2.1467(14), P4–P5 2.1700(13), P5–P6 2.2055(14), P6–H1P 1.38(5), P6–P7 2.2161(15), P7–P8 2.1348(18), P7–P11 2.165(2), P8–P9 2.118(2), P9–P10 2.094(3), P10–P11 2.155(3), P1–Fe1 2.3172(10), P2–Fe1 2.3325(10), P3–Fe1 2.3289(10), P4–Fe1 2.3248(10); P2-P1-P5 107.57(5), P3-P2-P1 103.63(5), P2-P3-P4 103.83(5), P3-P4-P5 107.77(5), P1-P5-P4 93.29(5), P1-P5-P6 108.94(6), P5-P6-P7 98.10(6).

detected by $^{31}$P NMR spectroscopy because the solubility of $NaNH_2$ is very low, and there is not enough $NH_2^-$ available in solution for further reaction.

The proposed reaction pathway is also based on the autometalation ability of $LiP(SiMe_3)_2$, which we studied a time ago.[17] Therefore, we selected $LiPH_2$ as a nucleophilic reagent, and an excess of **1** was reacted with $LiPH_2$ in THF at −60 °C. An immediate color change from green to deep red was observed. The $^{31}$P NMR spectrum of the reaction mixture show the formation of **5** as the main product with some unassigned impurities (Scheme 1). All attempts to isolate $[Li(THF)_x][\mathbf{5}]$ as a pure crystalline solid failed, but it can be precipitated with *n*-hexane as a solid in a 76% purity (determined by $^{31}$P NMR spectroscopy). The identity of **5** was confirmed by $^{31}P\{^1H\}$ NMR spectroscopy, in which an AMXX′YY′ spin system was observed with signals centered at −114.9, −40.5, 20.3, and 50.0 ppm. The presence of the $PH_2$ unit was unambiguously confirmed by $^{31}$P NMR spectroscopy and is attributed to the signal at −114.9 ppm. The other multiplets were assigned by $^{31}P,^{31}P$ COSY experiments. Furthermore, the simulated coupling constants for **5** are very similar to those found for **2**, **3**, and **4**. However, from a concentrated solution in THF, crystals of **6**, suitable for single-crystal X-ray diffraction, were obtained. As **6** was only isolated as a few crystals, unfortunately it could not be characterized further. All attempts to synthesize **6** directly and in higher yields failed. Note that all of the reported products **2**–**6** are extremely sensitive towards air and especially moisture.

DFT calculations show that the relative energy profile of the reaction of **1** with $PH_2^-$ differs considerably from that of the reaction of **1** with $NH_2^-$ (Figure 3). While the formation of **5** is exothermic by −72.4 kJ mol$^{-1}$, deprotonation of **5** to $[Cp^*Fe(\eta^4\text{-}P_5PH)]^{2-}$ (**B′**) is endothermic by 39.7 kJ mol$^{-1}$. Thus, the latter reaction is hampered, which allows the isolation of **5**. Furthermore, the deprotonation of **6** to the trianionic species $[\{Cp^*Fe(\eta^4\text{-}P_5)\}_2P]^{3-}$ (**D**) is also endothermic by 61.6 kJ mol$^{-1}$. These data clearly explain why, in the reaction of **1** with $NH_2^-$, **4** is obtained as final product, whereas for the reaction of **1** with $PH_2^-$, **5** is obtained as the main product.

The structure of $[Li_2(dme)_6][\mathbf{6}]$ was determined by single-crystal X-ray diffraction (Figure 4). In **6** two $[Cp^*Fe(\eta^4\text{-}P_5)]$ fragments are linked together by a PH unit with P–P distances corresponding to single bonds (P5–P6 2.2043(15) Å, P6–P7 2.155(15) Å). The P–P bond lengths within the $\eta^4$-$P_5$ unit are comparable with those found in **2**, with the exception of the P9–P10 bond, which is 2.096 Å, and thus slightly shorter than the corresponding bond length in **2** (P3–P4 2.1342(11) Å). The hydrogen atom attached to the atom P6 could be located from residual electron density map and refined with fixed thermal parameters.

In summary, we have shown that pentaphosphaferrocene is a reactive molecule, which is not only useful in coordination chemistry with transition metals but also reactive with different main-group nucleophiles. In this respect, it shows some similarities with its all-carbon relative ferrocene. However, in its reactivity **1** differs by undergoing transformations of the aromatic *cyclo*-$P_5$ ligand and forming unprecedented compounds with a $\eta^4$-$P_5$ structural pattern. Moreover, if H-containing nucleophiles are used, an aggregation of pentaphosphaferrocene molecules can yield di- and trianionic derivatives, revealing the ability of **1** to form novel aggregated and P-rich species. With these novel reactivity patterns, pentaphosphaferrocene becomes a valuable organometallic building block and opens a new chapter for its use in main-group chemistry.

Received: March 21, 2014
Published online: June 4, 2014

**Keywords:** density functional calculations · iron · main-group chemistry · nucleophilic attack · phosphorus

[1] T. J. Kealy, P. L. Pauson, *Nature* **1951**, *168*, 1039–1040.
[2] a) R. B. Woodward, M. Rosenblum, M. C. Whiting, *J. Am. Chem. Soc.* **1952**, *74*, 3458; b) R. A. Benkeser, D. Goggin, G. Schroll, *J. Am. Chem. Soc.* **1954**, *76*, 4025.
[3] N. J. Long, K. Kowalski, *Ferrocenes*, Wiley, Hoboken, **2008**, pp. 393–446.

  

[4] R. Gómez Arrayás, J. Adrio, J. C. Carretero, *Angew. Chem.* **2006**, *118*, 7836 – 7878; *Angew. Chem. Int. Ed.* **2006**, *45*, 7674 – 7715.
[5] M. F. R. Fouda, M. M. Abd-Elzaher, R. A. Abdelsamaia, A. A. Labib, *Appl. Organomet. Chem.* **2007**, *21*, 613 – 625.
[6] M. D. Rausch, D. J. Ciappenelli, *J. Organomet. Chem.* **1967**, *10*, 127.
[7] F. Rebiere, O. Samuel, H. B. Kagan, *Tetrahedron Lett.* **1990**, *31*, 3121 – 3124.
[8] J. Scherer, T. Brück, *Angew. Chem.* **1987**, *99*, 59; *Angew. Chem. Int. Ed. Engl.* **1987**, *26*, 59.
[9] a) M. Detzel, T. Mohr, O. J. Scherer, G. Wolmershäuser, *Angew. Chem.* **1994**, *106*, 1142 – 1144; *Angew. Chem. Int. Ed. Engl.* **1994**, *33*, 1110 – 1112; b) O. J. Scherer, *Acc. Chem. Res.* **1999**, *32*, 751 – 762.
[10] a) J. Bai, A. V. Virovets, M. Scheer, *Angew. Chem.* **2002**, *114*, 1808 – 1811; *Angew. Chem. Int. Ed.* **2002**, *41*, 1737 – 1740; b) M. Scheer, L. J. Gregoriades, A. V. Virovets, W. Kunz, R. Neueder, I. Krossing, *Angew. Chem.* **2006**, *118*, 5818 – 5822; *Angew. Chem. Int. Ed.* **2006**, *45*, 5689 – 5693.
[11] a) J. Bai, A. V. Virovets, M. Scheer, *Science* **2003**, *300*, 781 – 783; b) T. Li, J. Wiecko, N. A. Pushkarevsky, M. T. Gamer, R. Köppe, S. N. Konchenko, M. Scheer, P. W. Roesky, *Angew. Chem.* **2011**, *123*, 9663 – 9667; *Angew. Chem. Int. Ed.* **2011**, *50*, 9491 – 9495; c) M. Scheer, J. Bai, B. P. Johnson, R. Merkle, A. V. Virovets, C. E. Anson, *Eur. J. Inorg. Chem.* **2005**, 4023 – 4026; d) M. Scheer, A. Schindler, J. Bai, B. P. Johnson, R. Merkle, R. Winter, A. V. Virovets, E. V. Peresypkina, V. A. Blatov, M. Sierka, H. Eckert, *Chem. Eur. J.* **2010**, *16*, 2092 – 2107; e) M. Scheer, A. Schindler, C. Gröger, A. V. Virovets, E. V. Peresypkina, *Angew. Chem.* **2009**, *121*, 5148 – 5151; *Angew. Chem. Int. Ed.* **2009**, *48*, 5046 – 5049; f) M. Scheer, A. Schindler, R. Merkle, B. P. Johnson, M. Linseis, R. Winter, C. E. Anson, A. V. Virovets, *J. Am. Chem. Soc.* **2007**, *129*, 13386 – 13387; g) S. Welsch, C. Gröger, M. Sierka, M. Scheer, *Angew. Chem.* **2011**, *123*, 1471 – 1474; *Angew. Chem. Int. Ed.* **2011**, *50*, 1435 – 1438.
[12] R. F. Winter, W. E. Geiger, *Organometallics* **1999**, *18*, 1827 – 1833.
[13] M. V. Butovskiy, G. Balázs, M. Bodensteiner, E. V. Peresypkina, A. V. Virovets, J. Sutter, M. Scheer, *Angew. Chem.* **2013**, *125*, 3045 – 3049; *Angew. Chem. Int. Ed.* **2013**, *52*, 2972 – 2976.
[14] a) E. J. Padma Malar, *Eur. J. Inorg. Chem.* **2004**, 2723 – 2732; b) H. Krauss, G. Balazs, M. Bodensteiner, M. Scheer, *Chem. Sci.* **2010**, *1*, 337 – 342.
[15] D. Tofan, B. M. Cossairt, C. C. Cummins, *Inorg. Chem.* **2011**, *50*, 12349 – 12358.
[16] Owing to the limited solubility of $NaNH_2$ in dme, this reaction proceeds slowly, even at ambient temperature.
[17] a) M. Scheer, S. Gremler, E. Herrmann, U. Grünhagen, M. Dargatz, E. Kleinpeter, *Z. Anorg. Allg. Chem.* **1991**, *600*, 203 – 210; b) M. Scheer, S. Gremler, E. Herrmann, P. G. Jones, *J. Organomet. Chem.* **1991**, *414*, 337 – 349; c) M. Scheer, S. Gremler, E. Herrmann, M. Dargatz, H.-D. Schädler, *Z. Anorg. Allg. Chem.* **1993**, *619*, 1047 – 1052.

  